

The NeXT Mission

Tadayuki Takahashi^a, Richard Kelley^b, Kazuhisa Mitsuda^a, Hideyo Kunieda^c, Robert Petre^b, Nicholas White^b, Tadayasu Dotani^a, Ryuichi Fujimoto^d, Yasushi Fukazawa^e, Kiyoshi Hayashida^f, Manabu Ishida^a, Yoshitaka Ishisaki^g, Motohide Kokubun^a, Kazuo Makishima^h, Katsuji Koyamaⁱ, Greg M. Madejski^j, Koji Mori^k, Richard Mushotzky^b, Kazuhiro Nakazawa^h, Yasushi Ogasaka^c, Takaya Ohashi^g, Masanobu Ozaki^a, Hiroyasu Tajima^j, Makoto Tashiro^l, Yukikatsu Terada^l, Hiroshi Tsunemi^f, Takeshi Go Tsuruⁱ, Yoshihiro Ueda^m, Noriko Yamasaki^a, Shin Watanabe^a and the NeXT team

^aInstitute of Space and Astronautical Science (ISAS), JAXA, Kanagawa, 229-8510, Japan;

^bNASA/Goddard Space Flight Center, Greenbelt, MD 20771, USA;

^cDepartment of Physics, Nagoya University, Nagoya, 338-8570, Japan;

^dDepartment of Physics, Kanazawa University, Kanazawa, 920-1192, Japan;

^eDepartment of Physical Science, Hiroshima University, Hiroshia , 739-8526, Japan;

^fDepartment of Earth and Space Science, Osaka University, Osaka, 560-0043, Japan;

^gDepartment of Physics, Tokyo Metropolitan University, Tokyo, 192-0397, Japan;

^hDepartment of Physics, University of Tokyo, Tokyo, 113-0033, Japan;

ⁱDepartment of Physics, Kyoto University, Kyoto, 606-8502, Japan;

^jKAVLI Institute, Stanford University, Menlo Park, CA 94025, USA;

^kDepartment of Applied Physics, Miyazaki University, Miyazaki, 889-2192, Japan;

^lDepartment of Physics, Saitama University, Saitama, 338-8570, Japan;

^mDepartment of Astronomy, Kyoto University, Kyoto, 606-8502, Japan

ABSTRACT

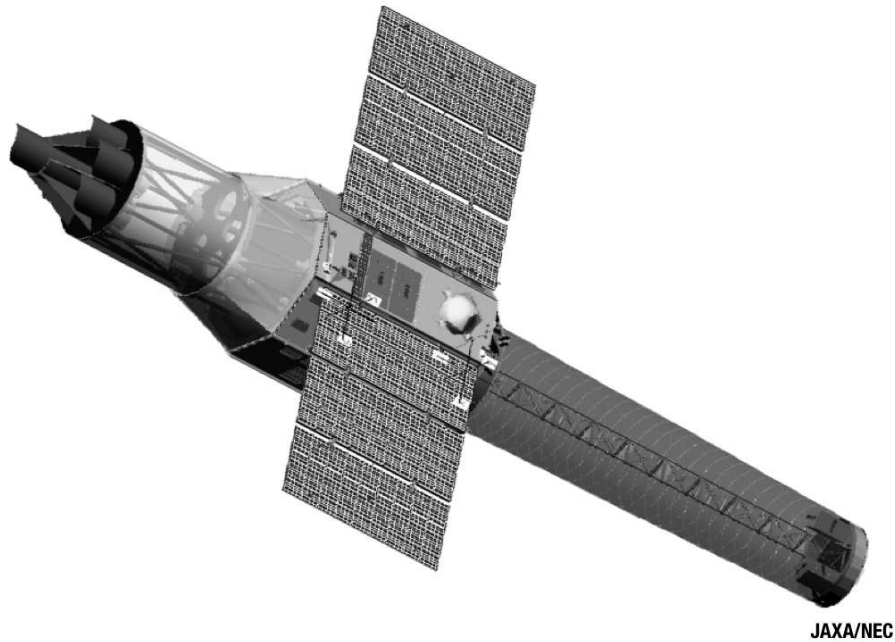
The NeXT (New exploration X-ray Telescope), the new Japanese X-ray Astronomy Satellite following Suzaku, is an international X-ray mission which is currently planned for launch in 2013. NeXT is a combination of wide band X-ray spectroscopy (3–80 keV) provided by multi-layer coating, focusing hard X-ray mirrors and hard X-ray imaging detectors, and high energy-resolution soft X-ray spectroscopy (0.3–10 keV) provided by thin-foil X-ray optics and a micro-calorimeter array. The mission will also carry an X-ray CCD camera as a focal plane detector for a soft X-ray telescope and a non-focusing soft gamma-ray detector. With these instruments, NeXT covers very wide energy range from 0.3 keV to 600 keV. The micro-calorimeter system will be developed by international collaboration lead by ISAS/JAXA and NASA. The simultaneous broad bandpass, coupled with high spectral resolution of $\Delta E \sim 7$ eV by the micro-calorimeter will enable a wide variety of important science themes to be pursued.

Keywords: X-ray, Hard X-ray, gamma-ray, X-ray Astronomy, Gamma-ray Astronomy

1. INTRODUCTION

The NeXT (New exploration X-ray Telescope) mission has been studied as the next key X-ray astronomy mission of Japan, which will be developed under international collaboration (see Fig. 1). It has completed the pre-phase A study in 2006 and entered into Phase A since June 2007. A Request For Proposal (RFP) for the spacecraft was released by ISAS/JAXA to Japanese industry in November 2007 and NEC was selected. In May, 2008, System Definition Review, which is required before entering Phase B, was completed. We anticipate that NeXT will enter Phase B in the middle of 2008 for the planned launch year of 2013. More recently, NASA has selected the

Send correspondence to T. Takahashi, E-mail: takahasi@astro.isas.jaxa.jp



JAXA/NEC

Figure 1. Artist's drawing of the NeXT satellite. The focal length of the Hard X-ray Telescope (HXT) is 12m, whereas the Soft X-ray Spectrometer (SXS) and Soft X-ray Imager (SXI) will have a focal length of 6 meters.

US participation in NeXT as a mission of opportunity. Under this program, the NASA/Goddard Space Flight Center will collaborate with ISAS/JAXA on the implementation of an X-ray microcalorimeter spectrometer.³

The NeXT mission objectives are to study the evolution of yet-unknown obscured super massive Black Holes (SMBHs) in Active Galactic Nuclei (AGN); trace the growth history of the largest structures in the Universe; provide insights into the behavior of material in extreme gravitational fields; determine the spin of black holes and the equation of state of neutron stars; trace particle acceleration structures in clusters of galaxies and SNRs; and investigate the detailed physics of jets.

In this paper, we will summarize the scientific requirements, the mission concept and the current baseline configuration of instruments of NeXT.

2. SCIENCE REQUIREMENTS

By comparison with the soft X-ray band, where the spectacular data from the previous X-ray satellites are revolutionizing our understanding of the universe below 10 keV, the sensitivities of hard X-ray missions flown so far have not dramatically improved over the last decade. The imaging capabilities at high X-ray energies open the completely new field of spatial studies of non-thermal emission above 10 keV. This will enable us to track the evolution of Active Galaxies with accretion flows which are heavily obscured, in order to accurately assess their contribution to the cosmic X-ray background over cosmic time. It will also allow us to map the spatial extent of the hard X-ray emission in diffuse sources, tracing the sites of particle acceleration structures in clusters of Galaxies and supernova remnants.⁶⁻⁸ Observing the hard X-ray synchrotron emission gives the maximum electron energy produced by the particle acceleration mechanism in SNR, while the high resolution SXS data on the gas kinematics of the SNR constrains the energy input into the accelerator.

In order to study the energy content of non-thermal emission and to draw a more complete picture of the high energy universe, observations by both a spectrometer with an extremely high resolution capable of measuring the bulk plasma velocities and/or turbulence with the resolution corresponding to the speed of a few $\times 100$ km/s and an arc-min imaging system in hard X-ray, with the sensitivity two-orders of magnitude better than previous

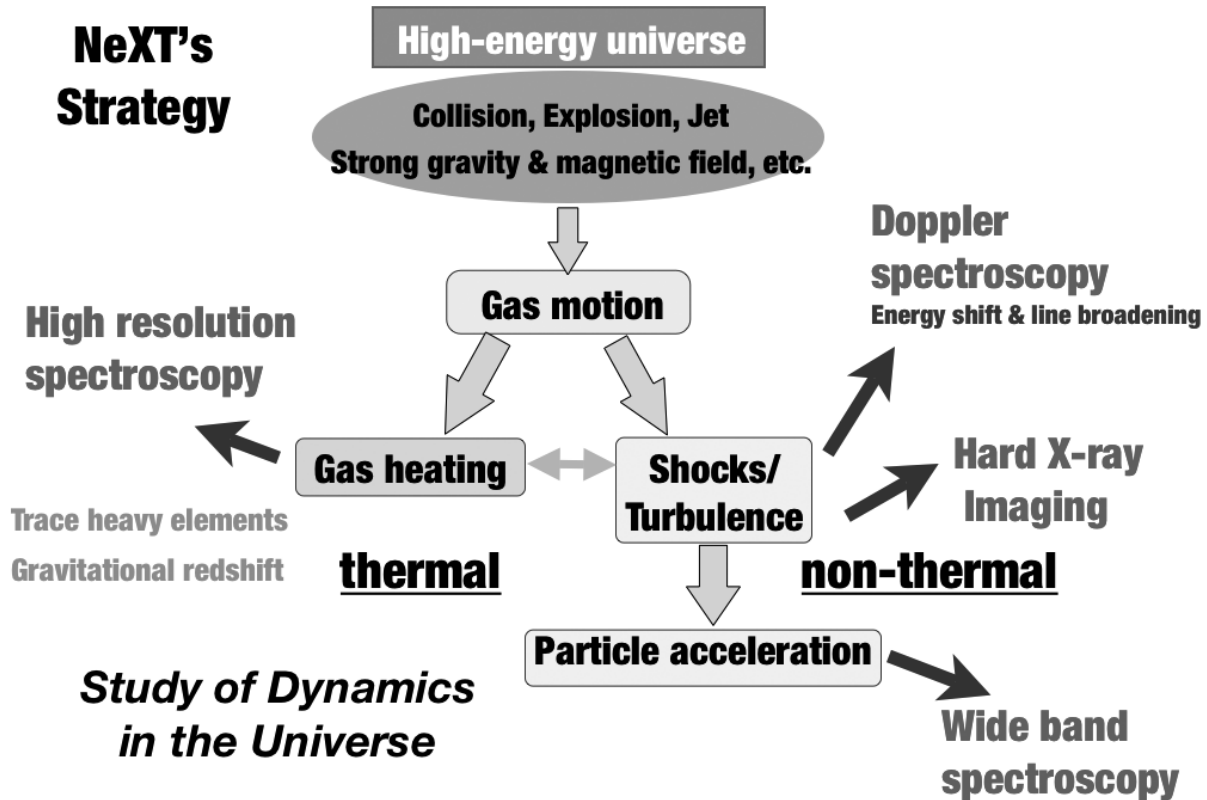


Figure 2. Strategy of the NeXT mission to study high energy universe. A set of detectors, which can perform (1) High resolution spectroscopy, (2) Doppler spectroscopy, (3) Hard X-ray imaging, and (4) Wide band spectroscopy, are required for the understanding of the high energy universe.

missions, are required (See Fig. 2). In clusters, X-ray hot gas is trapped in the gravitational potential well and shocks and/or turbulence are produced in this gas, as smaller substructures with their own hot gas halo fall into and merge with the dominant cluster. Large scale shocks can also be produced as gas from the intracluster medium falls into the gravitational potential of a cluster. Here there is a strong synergy between the hard X-ray imaging data and the high resolution (several eV) soft X-ray spectrometer which allows us to study the gas kinematics (bulk motion and turbulent velocity) via the width and energy of the emission lines. The kinematics of the gas provides unprecedented information about the bulk motion; the energy of this motion is in turn responsible for acceleration of particles to very high energies at shocks, which is in turn manifested via non-thermal processes, best studied via sensitive hard X-ray measurement.

On the smallest scales, many active galactic nuclei (AGN) show signatures from the innermost accretion disk in the form of broad “relativistic” Fe K emission lines. These broad lines were discovered using ASCA in the early 1990s and have been confirmed by XMM-Newton and Suzaku.^{9, 10} There is, however, a complex relationship between the Fe K line properties, the underlying continuum, and the signatures of cold and/or partially ionized material near the AGN. Precise measurements of the complex Fe K line and absorption components require high spectral resolution. Changes in the X-ray emission and absorption spectral features on the orbital time scale of black holes in AGN, enable characterization of the velocity field and ionization state of the plasma closest to the event horizon. The optically thick material that produces the broad fluorescent Fe K line also creates a Compton peak at $E > 20$ keV detectable with hard X-ray and soft gamma-ray detectors, providing multiple insights into the physics of the disk. In order to understand the evolution of environments surrounding super massive black holes, we need high signal-to-noise measurements of the broad lines of hundreds of AGN up to, at least, $z \sim 2$. This requires high spectral resolution and bandpass extending to at least ~ 40 keV. These observations will

Table 1. NeXT Mission

launch date	2013 (planned)
launch vehicle	JAXA H-IIA
orbit	550 km circular, <30 degree

provide the first unbiased survey of broad Fe K line properties across all AGN.

Precision cosmology uses astronomical observations to determine the large-scale structure and content of the Universe. Studies of clusters of galaxies have provided independent measurements of the dark energy equation of state and strong evidence for the existence of dark matter. Using a variety of techniques (including the growth of structure, the baryonic fraction in clusters, and the Sunyaev-Zel’dovich effect) a well-constructed survey of clusters of galaxies, with the necessary supporting data,¹¹ can provide precise measurements of cosmological parameters, including the amount and properties of dark energy and dark matter. The key is to connect observables (such as flux and temperature) to cluster mass. In the next few years, cluster surveys will be carried out by eROSITA, the South Pole Telescope, the Planck mission, and other Sunyaev-Zel’dovich Effect telescopes. To reduce the systematic uncertainties on the masses inferred from the coarser data from these surveys, a training set of precise cluster masses must be obtained. Measurements of bulk motion of cluster of galaxies and amounts of non-thermal energies going to cosmic-ray acceleration could reduce the “. . . substantial uncertainties in the baryonic physics which prevents their use at a high level of precision at the present time” (Dark Energy Task Force, Albrecht et al. 2006). Line diagnostics with energy resolution <7 eV greatly reduce the uncertainties in the baryonic physics by determining the velocity field, any deviations from thermal equilibrium, and an accurate temperature for each cluster. Information about the non-thermal particle content of the cluster can be determined via measurements of their Compton upscattering of the CMB: this is best studied via hard X-ray imaging, providing additional clues about the physical state of the cluster gas.

3. SPACECRAFT AND INSTRUMENTS

NeXT is designed to perform leading edge science with cutting edge technology. NeXT will carry two hard X-ray telescopes (HXTs) for the hard X-ray imager (HXI), and two soft X-ray telescopes (SXT), one with a micro-calorimeter spectrometer array with excellent energy resolution of ~ 7 eV, and the other with a large area CCD. In order to extend the energy coverage to soft γ -ray region, a Soft Gamma-ray Detector (SGD) will be implemented as a non-focusing detector. With these instruments, NeXT will cover the bandpass between 0.5 keV to 600 keV. The conceptual design of each instrument is shown in Fig. 3 and the specifications of instruments based on the base-line design are summarized in Table. 1 and 2.

Both soft and hard X-ray mirrors are mounted on top of the fixed optical bench. Two focal-plane detectors for soft X-ray mirrors are mounted on the base plate of the spacecraft, while two hard X-ray detectors are mounted on the extensible optical bench to attain 12 m focal length.

NeXT is in many ways similar to Suzaku in terms of orbit, pointing, and tracking capabilities, although the mass is larger; the total mass at launch will be 2400 kg. NeXT will be launched into a circular orbit with altitude 500–600 km, and inclination 30 degrees or less. Science operations will be similar to that of Suzaku, with pointed observation of each target until the integrated observing time is accumulated, and then slewing to the next target. A typical observation will require 40–100 ksec integrated observing time, which corresponds to 1–2.5 days of clock time. All instruments operate simultaneously.

3.1. Hard X-ray Imaging System

The hard X-ray imaging system onboard NeXT consists of two identical mirror-detector pairs (Hard X-ray Telescope (HXT) and Hard X-ray Imager (HXI)). The HXT has conical-foil mirrors with graded multilayer reflecting surfaces that provide a 5–80 keV energy range.¹⁵ The effective area of the HXT is maximised for a long focal length, with current design value of 12 m giving an effective area of ~ 300 cm² at 30 keV. A depth-graded multi-layer mirror reflects X-rays not only by total external reflection but also by Bragg reflection. In

Table 2. Specification of instruments (Requirements)

Hard X-ray Imaging System	HXT (Hard X-ray Telescope)/HXI (Hard X-ray Imager)	
	Focal Length	12 m
	Effective Area	300 cm ² (at 30 keV)
	Energy Range	5–80 keV
	Angular Resolution	<1.7 arcmin (HPD)
	Effective FOV	~9 × 9 arcmin (12 m Focal Length)
	Energy Resolution	< 1.5 keV (FWHM, at 60 keV)
	Timing Resolution	several 10 μs
	Detector Background	< 1–3 × 10 ⁻⁴ cts s ⁻¹ cm ⁻² keV ⁻¹
Operating Temperature	< -20 °C	
Soft X-ray Spectrometer System	SXT-S (Soft X-ray Telescope)/SXS (Soft X-ray Spectrometer)	
	Focal Length	6 m
	Effective Area	210 cm ² (at 6 keV)
	Energy Range	0.3–10 keV
	Angular Resolution	< 1.7 arcmin (HPD)
	Effective FOV	~ 3 × 3 arcmin
	Energy Resolution	<7 eV (FWHM, at 7 keV)
	Timing Resolution	several 10 μs
	Detector Background	<5 × 10 ⁻³ cts s ⁻¹ cm ⁻² keV ⁻¹
Operating Temperature	50 mK	
Soft X-ray Imaging System	SXT-I (Soft X-ray Telescope)/SXI (Sard X-ray Imager)	
	Focal Length	6 m
	Effective Area	360 cm ² (at 6 keV)
	Energy Range	0.3–12 keV
	Angular Resolution	< 1.7 arcmin (HPD)
	Effective FOV	~ 35 × 35 arcmin
	Energy Resolution	< 150 eV (FWHM, at 6 keV)
	Timing Resolution	4 sec
	Detector Background	< a few ×10 ⁻³ cts s ⁻¹ cm ⁻² keV ⁻¹
Operating Temperature	-120 °C	
Soft Gamma-ray non-Imaging System	SGD (Soft Gamma-ray Detector)	
	Energy Range	10 keV–600 keV
	Energy Resolution	2 keV (FWHM, at 40 keV)
	Effective Area	>200 cm ² Photo absorption mode (at 30 keV) >30 cm ² (Compton mode, at 100 keV)
	FOV	0.55 × 0.55 deg ² (< 150 keV) <10 × 10 deg ² (> 150 keV)
	Timing Resolution	several 10 μs
	Detector Background	< a few ×10 ⁻⁶ cts s ⁻¹ cm ⁻² keV ⁻¹ (100 – 200 keV)
	Operating Temperature	-20 °C

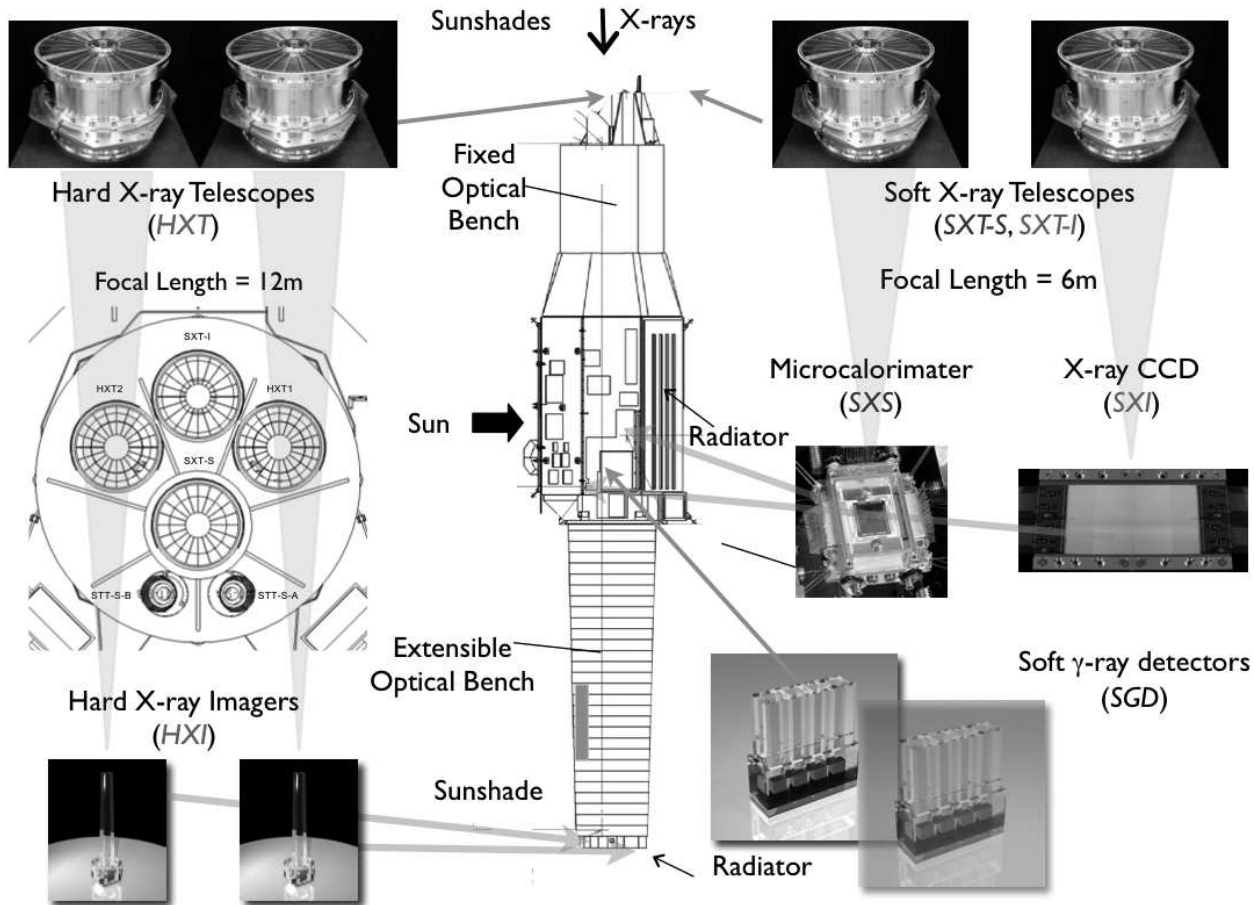


Figure 3. Configuration of the NeXT satellite

order to obtain high reflectivity up to 80 keV, the HXT's consist of a stack of multi-layers with different sets of periodic length and number of layer pairs with a carbon/platinum coating. The technology of a hard X-ray focusing mirror has already been proved by the balloon programs InFOC μ S (2001, 2004),¹³ HEFT (2004)¹⁴ and SUMIT (2006).¹³

The non-imaging instruments flown so far were essentially limited to studies of sources with 10–100 keV fluxes of at best $>10^{-12}$ – 10^{-11} erg cm $^{-2}$ s $^{-1}$. This limitation is due to the presence of high un-rejected backgrounds from particle events and Cosmic X-ray radiation, which increasingly dominate above 10 keV. Imaging, and especially focusing instruments have two tremendous advantages. Firstly, the volume of the focal plane detector can be made much smaller than for non-focusing instruments, so reducing the absolute background level since the background flux generally scales with the size of the detector. Secondly, the residual background, often time-variable, can be measured simultaneously with the source, and can be reliably subtracted. For these reasons, a focusing hard X-ray telescope in conjunction with an appropriate imaging detector sensitive for hard X-ray photons is the appropriate choice to achieve a breakthrough in sensitivity for the field of high energy astronomy.

The HXI consists of four-layers of 0.5 mm thick Double-sided Silicon Strip Detectors (DSSD) and one layer of 0.5–1 mm thick CdTe imaging detector (Fig. 5).^{16,17} In this configuration, soft X-ray photons will be absorbed in the Si part (DSSD), while hard X-ray photons go through the Si part and are detected by the newly developed CdTe double strip detector. With this configuration, the low energy spectrum, obtained with Si, is less contaminated with the background due to activation in heavy material, such as Cd and Te. Also we could use the depth information of interactions. Fast timing response of silicon strip detector and CdTe strip detector allows us to place the whole detector inside very deep well of the active shield made of BGO (Bi $_4$ Ge $_3$ O $_{12}$). Signal

from the BGO shield is used to reject background events. The total thickness of the four DSSDs is 2 mm, the same as that of the PIN detector of the HXD onboard Suzaku. The DSSDs cover the energy below 30 keV while the CdTe strip detector covers the 20-80 keV band. The DSSD has a size of $3 \times 3 \text{ cm}^2$ and a thickness of 0.5 mm, resulting in 2 mm in total. A CdTe strip detector has a size of $\sim 2 \times 2 \text{ cm}^2$ and a thickness of 0.5 mm. In addition to the increase of efficiency, the stack configuration and individual readout provide information on the interaction depth. This depth information is very useful to reduce the background in space applications, because we can expect that low energy X-rays interact in the upper layers and, therefore, we can reject low energy events detected in lower layers. Moreover, since the background rate scales with the detector volume, low energy events collected from the first few layers in the stacked detector have a high signal to background ratio, in comparison with events obtained from a monolithic detector with a thickness equal to the sum of all layers.

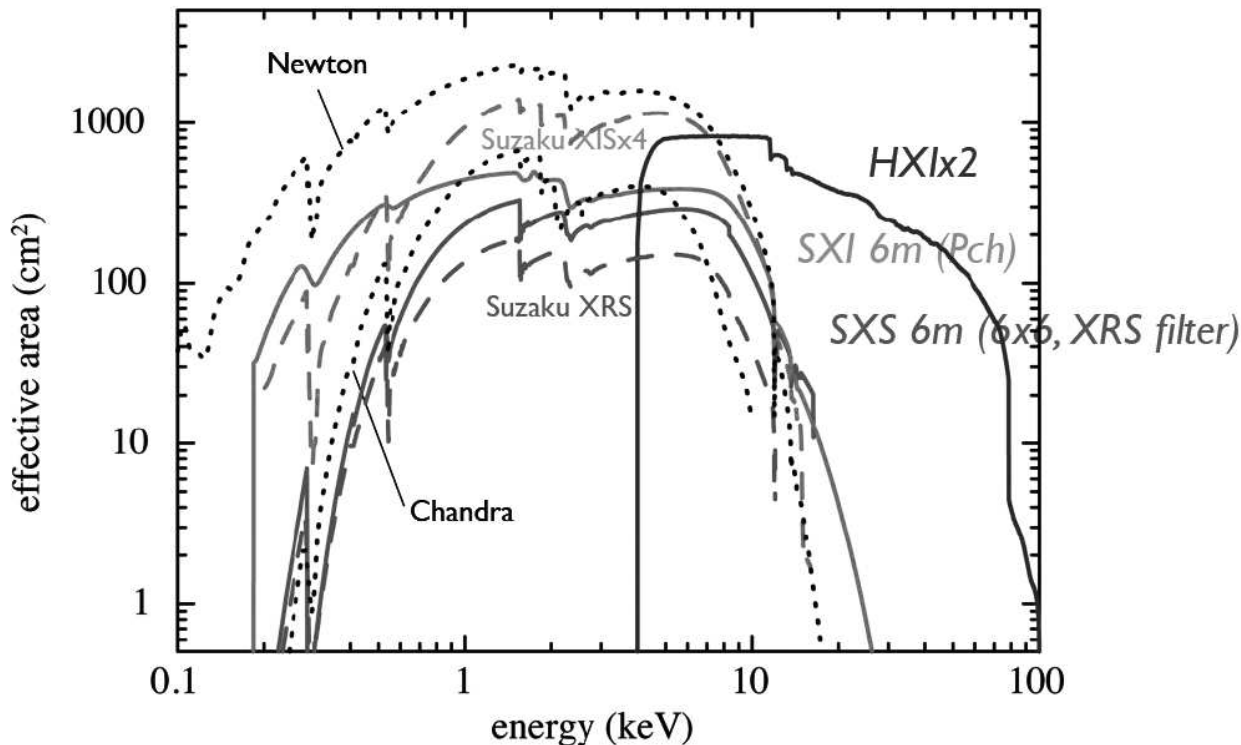


Figure 4. Effective Area of XRT telescopes for the NeXT mission

3.2. Soft X-ray Spectrometer System

The Soft X-ray Spectrometer (SXS) is based on Suzaku-XRS (X-Ray Spectrometer) technology, which is the lowest risk option for implementing the capabilities needed for the SXS. The SXS consists of the Soft X-ray Telescope (SXT-S), the X-ray Calorimeter Spectrometer (XCS) and the cooling system.¹⁸

The XCS is a 32 channel system with an energy resolution of $\leq 7 \text{ eV}$ between 0.3–12 keV. Micromachined, ion-implanted silicon is the basis of the thermistor array, and 8-micron-thick HgTe absorbers provide high quantum efficiency across the 0.3–12 keV band. With a 6-m focal length, the 0.83 mm pixel pitch corresponds to 0.48 arcmin, giving the array a field of view of 2.85 arcmin on a side. The detector assembly provides electrical, thermal, and mechanical interfaces between the detectors (calorimeter array and anticoincidence particle detector) and the rest of the instrument.

The SXS science objectives require a mirror with larger effective area than those flown on Suzaku, especially in the Fe K band. This is attained by the combination of increased focal length and larger diameter. The SXS effective area at 6 keV is 210 cm^2 , a 60 % increase over the Suzaku XRS, while at 1 keV the SXS has 160 cm^2 , a

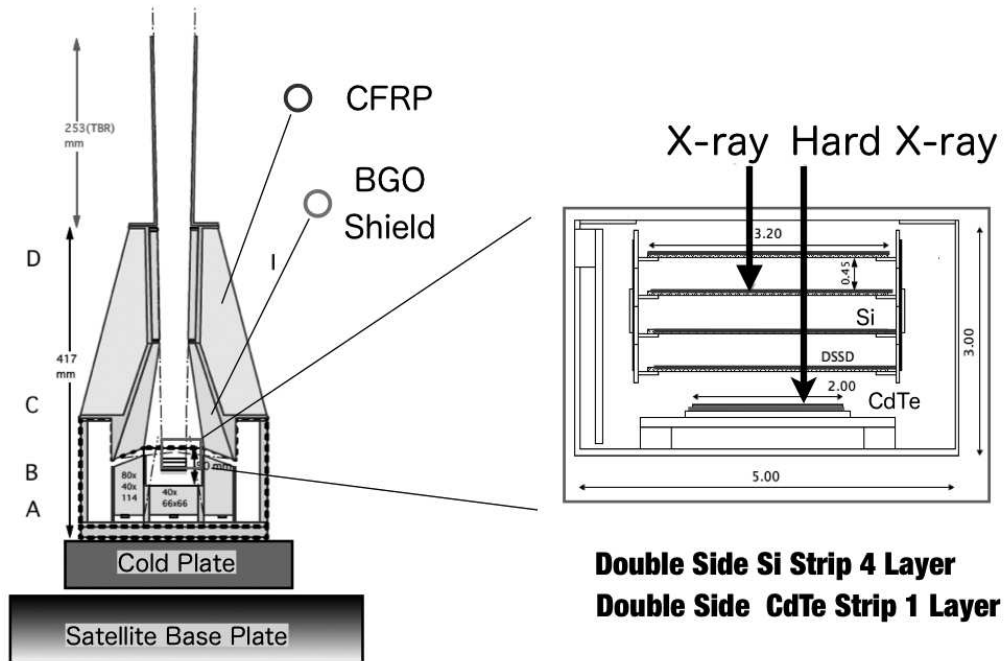


Figure 5. (left) Schematic drawing of the Hard X-ray Imager (HXI) (right) Cross section of the main detection part of the HXI, placed in a deep BGO active shield.

20 % increase. If we adopt a thin filter, the effective area at 1 keV increases to $\sim 250 \text{ cm}^2$. The required angular resolution is 1.7 arcmin, HPD, comparable to the orbit performance of the mirrors on Suzaku.

The XCS cooling system must cool the array to 50 mK with sufficient duty cycle to complete the SXS scientific objectives, requiring extremely low heat loads. To achieve the necessary gain stability and energy resolution, the cooling system must regulate the detector temperature to within $2 \mu\text{K}$ rms for at least 24 hours per cycle. As with Suzaku, the array will be cooled using an Adiabatic Demagnetization Refrigerator (ADR). This device is straightforward to construct, has no moving parts or sensitivity to gravity, and has strong flight heritage established by the XRS. The ADR and detector assembly will be developed, integrated, and tested together at GSFC, prior to installation into a redundant dewar system developed by ISAS. The ADR Controller (ADRC) electronics control and monitor the ADR performance.

For SXS, ISAS/JAXA will provide a redundant dewar system utilizing closed-cycle mechanical coolers that are not limited by expendables. This design is based on coolers developed for space-flight missions in Japan (Suzaku, Akari, and the SMILES instrument to be deployed on the ISS, Narasaki et al. 2005) that have achieved excellent performance with respect to cooling power, efficiency and mass. The 20 K thermal stage consists of a pair of redundant two-stage Stirling-cycle coolers. To provide the sub-2K heat-sink stage for the ADR, there is a hybrid, one-fault-tolerant system consisting of a LHe tank and a 3He Joule-Thomson (JT) refrigerator operating at 1.8 K. Under nominal operation, the JT cooler provides a 1.8 K thermal interface and maintains very low heat loads to the He tank. The helium reservoir ensures a high-heat-capacity thermal heat sink for the ADR. In the event that the JT cooler fails to operate, the He tank would become the primary heat sink (1.3 K) for the ADR; it is sized to last two years. Conversely, if the LHe supply is rapidly exhausted, the JT cooler would provide adequate cooling for science operations. A series of five blocking filters shield the calorimeter array from UV and longer wavelength radiation. The aluminized polyimide filters are identical to those successfully flown on Suzaku.

In combination with a high throughput X-ray telescope, SXS improves on the Chandra and XMM-Newton grating spectrometers in two important ways. At $E > 2 \text{ keV}$, SXS is both more sensitive and has higher resolution (Figs. 1.1 and 1.2), especially in the Fe K band where SXS has 10 times the collecting area and energy resolution,

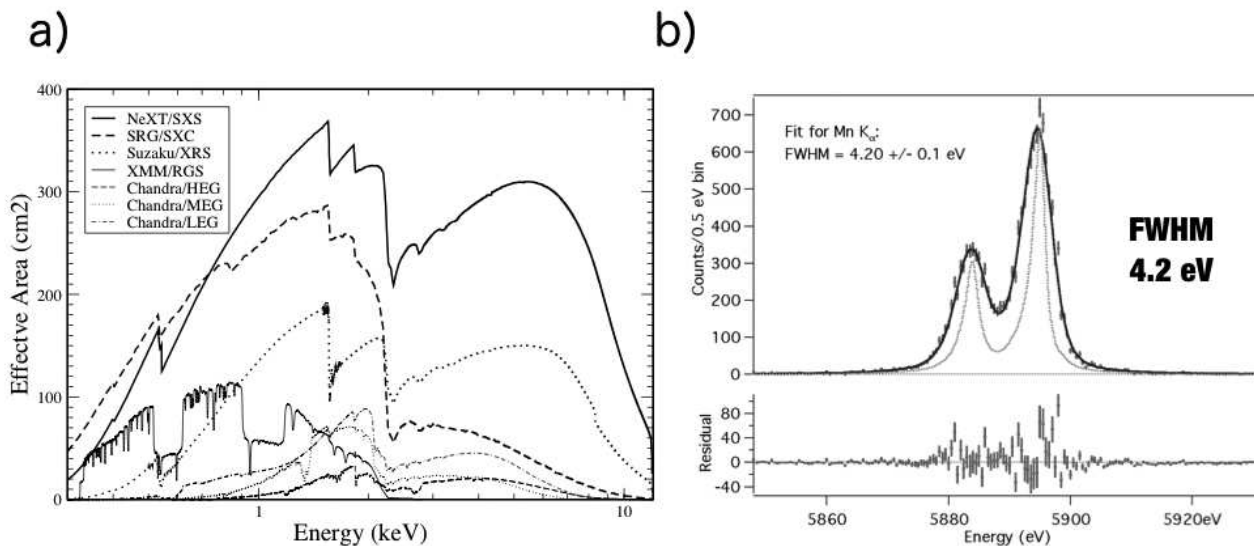


Figure 6. (a) The effective area of SXS (b) The energy resolution obtained from Mn $K\alpha_1$ using a detector from the XRS program but with a new sample of absorber material (HgTe) that has lower specific heat, leading to an energy resolution of 4.2 eV (FWHM). The SXS could have an energy resolution approaching this value (see Kelley et al 2007).

giving a net improvement in sensitivity by a factor of 30 over Chandra. The broad bandpass of SXS encompasses the critical inner-shell emission and absorption lines of Fe I-XXVI between 6.4 and 9.1 keV. Fe lines are useful because of their (1) strength, due to the high abundance and large fluorescent yield (30%), (2) spectral isolation from other lines, and (3) relative simplicity of the atomic physics. Fe K emission lines reveal conditions in plasmas with temperatures between 10^7 and 10^8 K, typical values for stellar accretion disks, SNRs, clusters of galaxies, and many stellar coronae. In cooler plasmas, Si, S, and Fe fluorescence and recombination occurs when an X-ray source illuminates nearby neutral material. Fe emission lines provide powerful diagnostics of non-equilibrium ionization due to innershell K-shell transitions from Fe XVII–XXIV.¹²

SXS uniquely performs high-resolution spectroscopy of extended sources. In contrast to a grating, the spectral resolution of the calorimeter is unaffected by source size because it is non-dispersive. For sources with angular extent larger than 10 arcsec, Chandra MEG resolution is degraded to that of a CCD; that of the XMM-Newton RGS is similarly degraded for sources with angular extent ≥ 2 arcmin. SXS makes possible high-resolution spectroscopy of sources inaccessible to current grating instruments.

The key properties of SXS are its high spectral resolution for both point and diffuse sources over a broad bandpass (≤ 7 eV FWHM throughout the 0.3–12 keV band), high sensitivity (effective area of 160 cm² at 1 keV and 210 cm² at 7 keV), and low non-X-ray background (1.5×10^{-3} cts s⁻¹keV⁻¹). These properties open up the full range of plasma diagnostics and kinematic studies of X-ray emitting gas for thousands of targets, both Galactic and extragalactic. SXS improves upon and complements the current generation of X-ray missions, including Chandra, XMM-Newton, Suzaku and Swift.

3.3. Soft X-ray Imaging System

X-ray sensitive silicon charge-coupled devices (CCDs) are a key device for the X-ray astronomy. The low background and high energy resolution achieved with the XIS/Suzaku clearly show that the X-ray CCD will also play very important role in the NeXT mission. Soft X-ray imaging system consists of an imaging mirror and a CCD camera (Soft X-ray Telescope (SXT-I) and Soft X-ray Imager (SXI)).^{20, 21}

In order to cover the soft X-ray band below 10 keV, the SXI will use next generation Hamamatsu CCD chips with a thick depletion layer, low noise, and almost no cosmetic defects. The SXI features a large FOV and covers 35×35 arcmin² region on the sky, complementing the smaller FOV but much higher spectral resolution

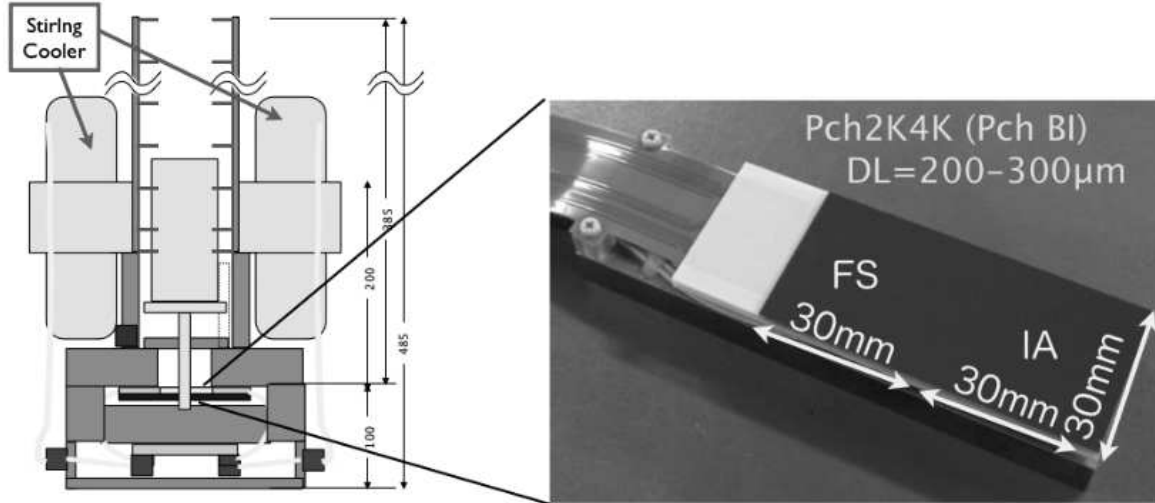


Figure 7. Schematic drawing of the Soft X-ray Imager (SXI) and a picture of a prototype CCD chip).

of the SXS calorimeter. A mechanical cooler ensures a long operational life at $-120\text{ }^{\circ}\text{C}$. The overall quantum efficiency and spectral resolution is better than the Suzaku XIS. The imaging mirror has a 6-m focal length, and a diameter no larger than 45 cm.

3.4. Soft Gamma-ray Detector (SGD)

Highly sensitive observations in the energy range above the HXT/WXI bandpass are crucial to study the spectrum of accelerated particles. The SGD is a non-focusing soft gamma-ray detector with a 10–600 keV energy range and sensitivity at 300 keV, more than 10 times better than the Suzaku HXD (Hard X-ray Detector). It outperforms previous soft- γ -ray instruments in background rejection capability by adopting a new concept of narrow-FOV Compton telescope.^{22, 23}

In order to lower the background dramatically and thus to improve the sensitivity as compared to the HXD of Suzaku, we combine a stack of Si strip detectors and CdTe pixel detectors to form a Compton telescope. The telescope is then mounted inside the bottom of a well-type active shield. Above ~ 50 keV, we can require each event to interact twice in the stacked detector, once by Compton scattering in a stack of Si strip detectors, and then by photo-absorption in the CdTe part (Compton mode). Once the locations and energies of the two interactions are measured, the Compton kinematics allows us to calculate the energy and direction (as a cone in the sky) of the incident γ -ray by following the Compton equation,

As shown schematically in Fig. 8 (right), the telescope consists of 32 layers of 0.6 mm thick Si pad detectors and eight layers of thin CdTe pixellated with a thickness of 0.75 mm. The sides is also surrounded by two layers of CdTe pixel detectors. The opening angle provided by the fine collimator is 0.5 degree and by the BGO shield is ~ 10 degrees at 500 keV, respectively. As compared to the HXD, the shield part is made compact by adopting the newly developed avalanche photodiode. An additional copper collimator restricts the field of view of the telescope to 30° for low energy photons (< 100 keV) to minimize the flux due to the Cosmic X-ray Background from the FOV. These modules are then arrayed to provide the required area (Fig. 8 (left)). We will have two SGD detectors each consisted of four units. Each detector will be mounted separately on two sides of the satellite. It should be noted that when the Compton condition is not used (Photo absorption mode), the stacked DSSD can be used as an usual photo-absorption type detector with the total thickness ~ 20 mm of silicon. The detector then covers from 10 keV as a collimator-type γ -ray detector. The effective area of the SGD is $> 30\text{ cm}^2$ at 150 keV in the Compton mode and $> 200\text{ cm}^2$ at 30 keV in the Photo absorption mode. Since the scattering angle of gamma-rays can be measured when we reconstruct the Compton scattering in the Compton camera, the SGD will also be sensitive to the polarization of the incident γ -rays.²⁴

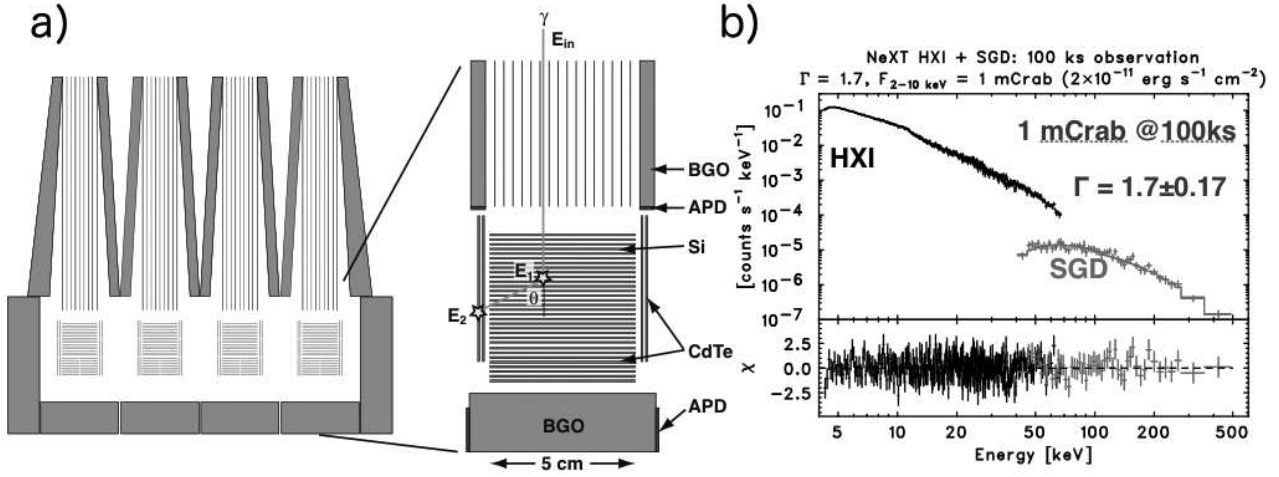


Figure 8. (a) Schematic drawing of the Soft Gamma-ray Detector (SGD). (b) Simulated spectrum of 1 mCrab hard X-ray source for the observation time of 100 ksec.

4. EXPECTED PERFORMANCE

With NeXT, we expect to achieve an area of about 300 cm^2 at 30 keV with a typical angular resolution of $60''$ (HPD). Fig. 9 shows Detection limits of the SXT-I/SXI and HXT/HXI for point sources and for sources with of $60' \times 60'$ extension. By assuming a background level of $\sim 1 \times 10^{-4} \text{ counts/s/cm}^2/\text{keV}$, in which the non X-ray background is dominant, the source detection limit in 1000 ksec would be roughly $10^{-14} \text{ erg cm}^2 \text{ s}^{-1}$ in terms of the 10–80 keV flux for a power-law spectrum with a photon index of 2. This is about two orders of magnitude better than present instrumentation, so will give a breakthrough in our understanding of hard X-ray spectra. With this sensitivity, 40-50 % of hard X-ray Cosmic Background would be resolved.²⁵

In addition to the imaging observations below 80 keV, the SGD will provide a high sensitivity in the soft γ -ray region to match the sensitivity of the HXT/HXI combination. The extremely low background brought by the new concept of a narrow-FOV Compton telescope adopted for the SGD will provide sensitive γ -ray spectra up to 600 keV, with moderate sensitivity for polarization measurements.

SXS spectroscopy of extended sources can reveal line broadening and Doppler shifts due to turbulent or bulk velocities (Fig. 10). This capability enables the spectral identification of cluster mergers, SNR ejecta dispersal patterns, the structure of AGN and starburst winds, and the spatially dependent abundance pattern in clusters and elliptical galaxies. SXS can also measure the optical depths of resonance absorption lines, from which the degree and spatial extent of turbulence can be inferred. Additionally, SXS can reveal the presence of relatively rare elements in SNRs and other sources through its high sensitivity to low equivalent width emission lines. The low SXS background ensures that the observations of almost all line rich objects will be photon limited rather than background limited.

XMM-Newton and Suzaku spectra frequently show time-variable absorption and emission features in the 5–10 keV band. If these features are due to Fe, they represent gas moving at very high velocities with both red and blue shifted components from material presumably near the event horizon. CCD resolution is too low and the required grating exposures are too long to properly characterize the velocity field and ionization of this gas and determine whether it is from close to the black hole or from high velocity winds. SXS, in combination with HXI, provides a dramatic increase in sensitivity over Suzaku, enabling measurements that probe the geometry of the central regions of ~ 50 AGNs on the orbital timescale of the Fe producing region (for an AGN with a $3 \times 10^7 M_{\odot}$ black hole, this is $\sim 60 GM_{\odot}/c^2 = 10 \text{ ksec}$).

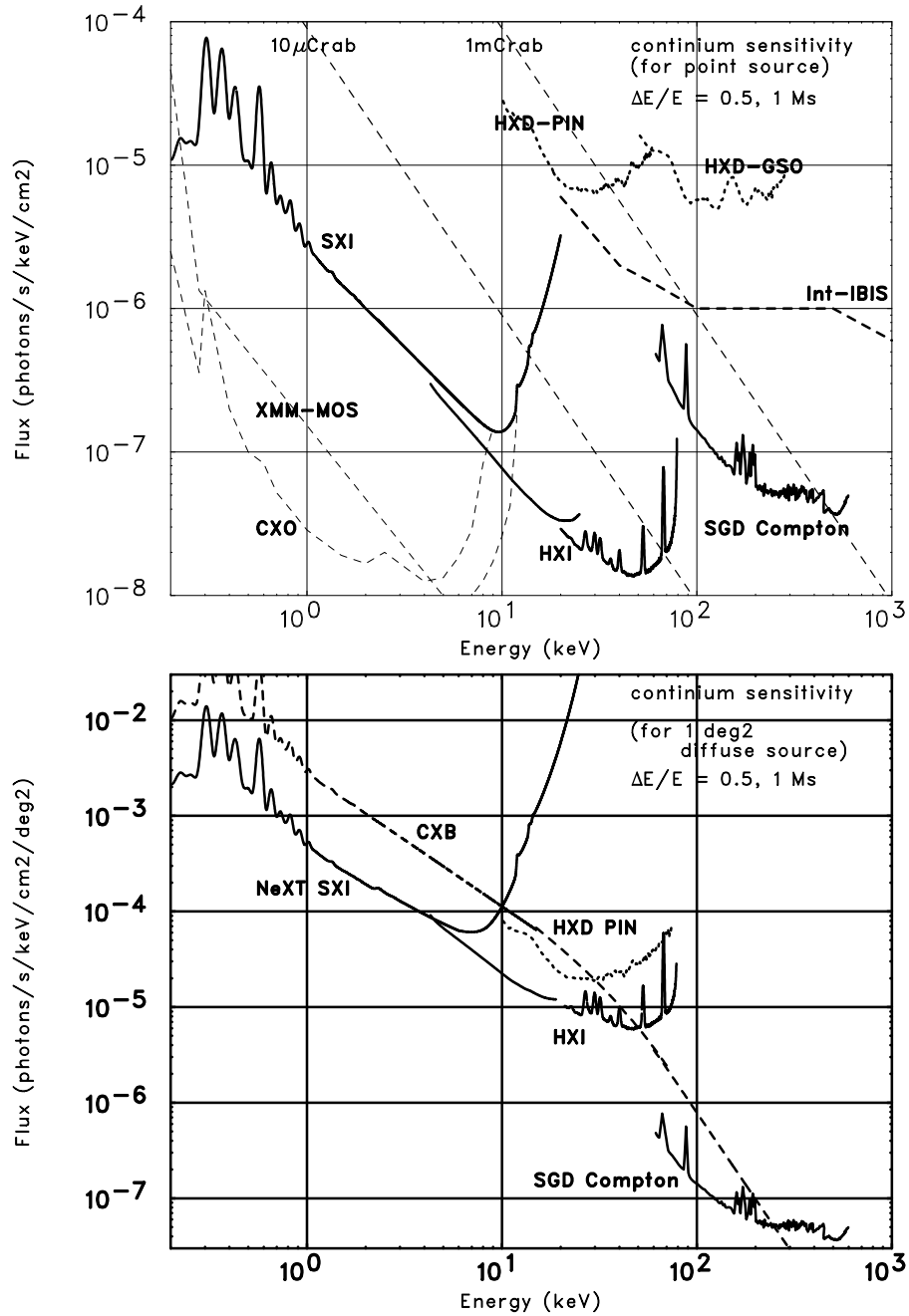


Figure 9. Detection limits of the SXT-I/SXI and HXT/HXI for (a) point sources and (b) for sources with of 1 \times 1 deg² extension (bottom) as functions of X-ray energy, where the spectral binning with $\Delta E/E = 0.5$ and 1000 ksec exposure are assumed. Detection limits for the XMM-Newton, Chandra, Suzaku and Integral observatories are shown for comparison for the sensitivity for point sources.

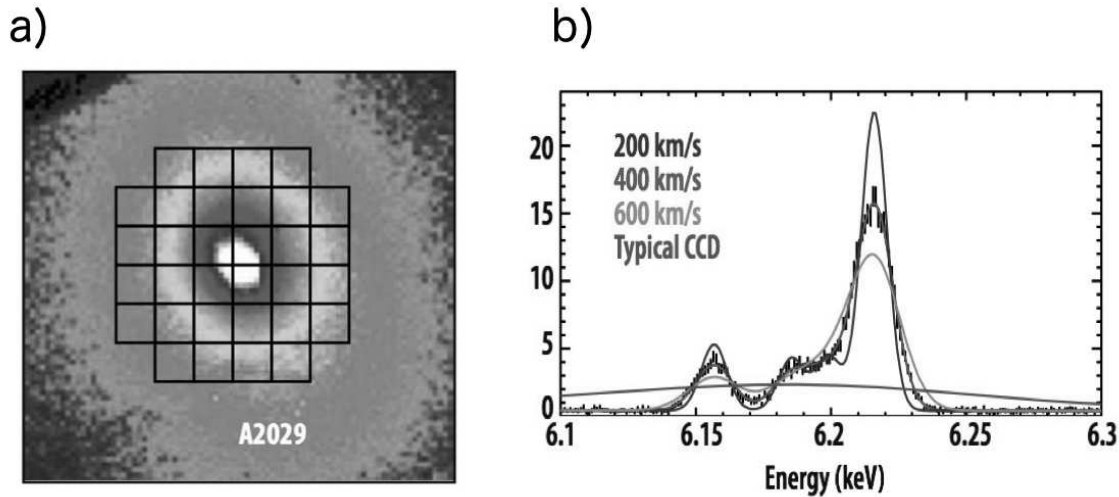


Figure 10. A portion of a simulated spectrum from the cluster A2029, assuming 400 km/s turbulence, and models assuming 200, 400, and 600 km/s, clearly showing the capability of SXS to measure cluster dynamics. The simulation is for 100 ksec.

Acknowledgement

The authors are deeply grateful for on-going contributions provided by other members in the NeXT team in Japan and the US: L. Angelini, N. Anabuki, K. Arnaud, H. Atsukade, H. Awaki, A. Banba, M. Bautz, G. Brown, K.-W. Chan, J. Cottam, J. P. Doty, Y. Ezoe, A. Furusawa, F. Furusawa, M. Galeazzi, K. Gendreau, Y. Haba, K. Hamaguchi, I. Harrus, T. Hashimoto, J. Hiraga, A. Hornschemeier, U. Hwang, N. Isobe, M. Itoh, T. Kallman, H. Katagiri, J. Kataoka, M. Kawaharada, N. Kawai, C. Kilbourne, S. Kitamamo, T. Kohmura, M. Kokubun, A. Kubota, J. Lochner, M. Loewenstein, Y. Maeda, H. Matsumoto, D. McCammon, K. Matsumoto, T. Mihara, E. Miyata, T. Mizuno, H. Mori, K. Mori, K. Mukai, H. Murakami, M. Murakami, T. Murakami, Y. Nakagawa, H. Nakajima, M. Nakajima, M. Nomachi, T. Numasawa, T. Okajima, N. Ohta, F. S. Porter, I. Sakurai, R. Sambruna, K. Sato, A. Senda, P. Serlemitsos, K. Shinozaki, R. Smith, Y. Soong, H. Sugita, M. Suzuki, A. Szymkowiak, H. Takahashi, T. Tamagawa, T. Tamura, T. Tanaka, Y. Tawara, Y. Terashima, H. Tomida, Y. Uchiyama, S. Ueno, S. Uno, Y. Urata, K. Yamaoka, H. Yamashita, M. Yamauchi, S. Yamauchi, D. Yonetoku, and A. Yoshida.

REFERENCES

1. NeXT Satellite Proposal, the NeXT working group, submitted to ISAS/JAXA (2005)
2. NeXT Satellite Proposal, the NeXT working group, submitted to ISAS/JAXA (2003)
3. SXS Proposal, "High Resolution X-ray Spectroscopy for the JAXA New Exploration X-ray Telescope", NASA/GSFC, submitted to NASA (2007)
4. H. Kunieda, "Hard X-ray Telescope Mission (NeXT)," Proc. SPIE, vol. 5488, p. 187 (2004)
5. T. Takahashi, K. Mitsuda, & H. Kunieda, "The NeXT Mission," Proc. SPIE, Volume 6266, p. 62660D (2006)
6. K. Koyama et al., "Evidence for Shock Acceleration of High-Energy Electrons in the Supernova Remnant SN:1006," Nature, 378, 255 (1995)
7. Y. Uchiyama, F. Aharonian, T. Tanaka, T. Takahashi, Y. Maeda, "Extremely fast acceleration of cosmic rays in a supernova remnant," Nature, 449, 576 (2007)
8. F. A. Aharonian, F., Very high energy cosmic gamma radiation: A crucial window on the extreme universe, World Scientific (2004)

9. Y. Tanaka, et al., "Gravitationally Redshifted Emission Implying an Accretion Disk and Massive Black-Hole in the Active Galaxy MCG:-6-30-15," *Nature*, 375, 659 (1995)
10. J.N. Reeves et al., "Revealing the High Energy Emission from the Obscured Seyfert Galaxy MCG-5-23-16 with Suzaku," *PASJ*, 59S, 301 (2007)
11. D. Rapetti, S. Allen, A. Mantz, "The prospects for constraining dark energy with future X-ray cluster gas mass fraction measurements," *MNRAS*, 2008, in press.
12. V. Decaux et al., "High Resolution Measurement of the K_{α} Spectrum of Fe XXV-XVIII: New Spectral Diagnostics of Nonequilibrium Astrophysical Plasmas," *ApJ*. 482, 1076-1084 (1997)
13. H. Kunieda et al., "Balloon-borne hard X-ray Imaging Observation of non-thermal phenomena", *Proc. SPIE*, 6266, 62660B (2006)
14. F. Harrison et al., "Development of the High-Energy Focusing Telescope (HEFT) Balloon Experiment," *Proc. SPIE*, 4012, 693 (2000)
15. Y. Ogasaka et al., "The NeXT x-ray telescope system: status update", in these proceedings.
16. K. Nakazawa et al., "Hard X-ray Imager for the NeXT Mission", *Proc. SPIE*, 6266, p. 62662H (2006)
17. M. Kokubun et al., "Hard X-ray imager (HXI) for the NeXT mission", in these proceedings.
18. K. Mitsuda et al. "The X-ray microcalorimeter on the NeXT mission", in these proceedings.
19. R.L. Kelley, C.A. Allen, M. Galeazzi, C.A. Kilbourne, D. McCammon, F.S. Porter, and A.E. Szymkowiak, "Ion-implanted Silicon X-Ray Calorimeters: Present and Future", *J. Low Temp. Phys.*, Vol. 151, Nos. 1-2 (April 2008)
20. T. G. Tsuru et al., "Soft X-ray Imager (SXI) onboard the NeXT satellite", *Proc. SPIE*, 6266, p. 62662I (2006)
21. H. Tsunemi et al., "The SXI: CCD camera onboard the NeXT mission", in these proceedings.
22. T. Takahashi, T. Kamae, and K. Makishima, "Future Hard X-ray and Gamma-ray Observations." in *New Century of X-ray Astronomy*, ASP 251 210 (2002)
23. T. Takahashi et al., "Wide band X-ray Imager (WXI) and Soft Gamma-ray Detector (SGD) for the NeXT Mission," *Proc. SPIE*, vol. 5488, pp.549-560 (2004)
24. H. Tajima, T. Mitani, T. Tanaka, H. Nakamura, T. Nakamoto, K. Nakazawa, T. Takahashi, Y. Fukazawa, T. Kamae, M. Kokubun, G. Madejski, D. Marlow, M. Nomachi, E. do Couto e Silva, "Gamma-ray polarimetry with Compton Telescope," *Proc. SPIE*, vol. 5488, pp. 561-571 (2004)
25. Y. Ueda et al., "Cosmological Evolution of the Hard X-Ray Active Galactic Nucleus Luminosity Function and the Origin of the Hard X-Ray Background", *ApJ*, 598, 886 (2003)